THE NATIONAL UNIVERSITY OF
SCIENCE AND TECHNOLOGY
POLITEHNICA BUCHAREST

DOCTORAL SCHOOL OF
ELECTRICAL ENGINEERING

# DOCTORAL THESIS

## THE USE OF RENEWABLE ENERGY SOURCES IN MARINE CLIMATE AREAS

**Scientific Advisor:**

**Professor PhD Engineer Mihai Octavian POPESCU**

**Doctoral Student:**

**Engineer Mihai BĂLĂCEANU**

**BUCHAREST**

**2024**

# TABLE OF CONTENTS

**Chapter I Introduction** 4
1.1 Marine climate zones and ecological responsibility 4
1.2 Thesis objectives 5
1.3 Thesis structure 6
**Chapter II Utilization of renewable energy sources in marine climate zones** 8
2.1 Renewable energies in marine climate zones 8
2.2 Photovoltaic cells and their operating principle 15
2.2.1 General information and structure 15
2.2.2 Types of photovoltaic panels 21
2.2.3 Photovoltaic systems 22
2.2.4 Solar irradiation 24
2.2.5 Photovoltaic cell parameters 27
2.2.6 Importance of solar energy in marine climate zones 29
2.3 Conclusions and contributions 30
**Chapter III Influence of the marine environment on photovoltaic systems** 32
3.1 Climate. Variability and predictability 32
3.1.1 Recent climate trends 32
3.1.2 Environmental factors influencing PV panel performance 35
3.1.3 Effects of solar irradiance and its variability 36
3.1.4 Effects of temperature on PV panels 38
3.1.5 PV panel cooling techniques 40
3.1.6 Effects of humidity on PV panel efficiency 43
3.1.7 Dust 43
3.2 Wind analysis 44
3.2.1 Effects of wind intensity on PV Panel efficiency 44
3.3 Marine-coastal environment and its impact on PV panels 45
3.3.1 Corrosion/effects of salinity 45
3.3.2 Effects of weather conditions on PV panels 47
3.4 Conclusions and contributions 48
**Chapter IV Influence of environmental factors on a photovoltaic panel installed in a coastal marine environment** 50
4.1 Influence of environmental factors on a photovoltaic panel – PVsyst and LabVIEW simulation 50
4.1.1 Description of the PVsyst program 51
4.1.2 Shockley Mathematical Model 53
4.1.3 Wind speed in PVsyst 54
4.1.4 Influence of environmental factors – PVsyst simulation 55
4.2 Influence of environmental factors/mathematical model 68
4.2.1 General information. mathematical model 68
4.3 LabVIEW simulation of a PV panel with a maximum power of 10 Wp 71
4.3.1 Description of the LabVIEW program 71
4.3.2 LabVIEW simulation to observe the impact of ambient temperature and wind speed on PV panel efficiency 73

4.4 Conclusions and contributions 79
**Chapter V Analysis of experimental results and impact of the marine environment on the efficiency of a 10 Wp PV panel installed on the coast** 82
5.1 Description of the experimental stand 82
5.1.1 Components and characteristics of the stand 82
5.2 Acquisition and analysis of experimental data for a 10 Wp PV panel 86
5.2.1 Acquired data and correlation with simulated data 86
5.2.2 Data analysis for a short period with maximum efficiency 90
5.3 Influence of air humidity on the efficiency of the experimental stand 93
5.3.1 Description of the experimental stand for measuring relative humidity and data analysis 93
5.4 Conclusions and contributions 97
**Chapter VI Conclusions and contributions** 98
**Bibliography** 103

## 1. Maritime Climate Zones and Ecological Responsibility

As the cost of conventional energy continues to rise and environmental concerns intensify, there is a growing interest in renewable energy. It is believed that conventional energy will only be available for another 50 years, making it essential to find a renewable energy source that is safe and feasible to replace fossil fuels. Solar energy is a superior alternative to conventional energy because it is renewable and produces green energy that can be used directly. The maritime industry has become a leader in raising awareness of environmental issues, driven by the urgent need to reduce carbon emissions from ships. This suggests that the maritime sector has recognized the negative impact of its activities on the environment and has begun to take measures to reduce its contribution to pollution, particularly by decreasing its carbon footprint. On this journey towards sustainability, solar energy has emerged as a lifeline, harnessing the inexhaustible power of the Sun to free ships and port sectors from their dependence on fossil fuels. Technological advances have made solar energy more accessible and widely used both in coastal areas and on large ships and small boats.

Evaluating the economic feasibility and long-term profitability of implementing PV energy on different types of ships and port areas is an evolving field of study. Further research is urgently needed to obtain a comprehensive overview of the return on investment, operating expenses, and potential economic obstacles that could influence the widespread adoption of these technologies.

## 2. Renewable Energies in Maritime Climate Zones

Since ancient times, humans have settled in areas bathed by the waters of rivers, seas, and oceans. The reasons are easy to understand, considering that the human attraction to water regions has been deeply rooted in fundamental human needs. This has led to the formation of significant settlements along waterways and on the shores of seas and oceans around the world. Historical data attest to the development of shipbuilding beginning in the 3rd millennium BC in various regions of the world, with particular emphasis on cultural centers in the Mediterranean Sea and Northern Europe. Here, we can mention ancient civilizations such as the Egyptian, Mesopotamian, and not least the Phoenician population, who played a significant role in the development of maritime transport.

When discussing waterway transport, it is important to remember the significant advantages in terms of transport costs, market share, and ton-mile capacity.

Despite the many advantages of waterway transport, it also represents a major source of pollution.

The production of greenhouse gases in the atmosphere leads to climate and environmental changes. In 2020, a reduction in carbon dioxide released into the atmosphere was recorded, due to the SARS-COV-2 virus pandemic. However, the near future predicts a significant increase in these types of gases, with maritime transport considered a primary source for the release of greenhouse gases into the atmosphere. Port operations (vehicles serving port areas as well as various port installations equipped with internal combustion engines) and the operation of ships both in port and at anchor play a major role in air pollution in the maritime sector.

To decarbonize the waterway transport industry, it is clear that low-carbon emission technologies need to be implemented, with a particular focus on alternative fuels, renewable energy sources, and shore-based energy supply sources.

**The Aquaris Marine Renewable Energy** (MRE) system is an integrated system of rigid sails, photovoltaic panels, energy storage modules, and a network of computers that allow ships to capture and transform renewable energies (solar and wind energy) into electricity. A central software commands the automatic positioning of the sails to best suit the prevailing weather conditions, and these can then be safely lowered and stored when the sea does not permit their use (strong winds, heavy precipitation)[1]. This system can also be used while the ship is stationary (at anchor or in port).

## 2.1 Photovoltaic Cells and Operating Principle

**Energy Bands**

An electron possesses a negative electric charge, while a proton possesses a positive electric charge. These two electric charges are equal in magnitude but opposite in sign. Scientists have measured the mass and size of these two particles to determine the amount of electric charge each holds. Although the mass of a proton is approximately 1827 times greater than the mass of an electron, both particles have the same amount of electric charge.

The third particle we encounter in an atom is the neutron. Its mass is roughly equal to that of the proton, but it is electrically neutral.

According to theory, the protons, neutrons, and electrons in atoms are arranged similarly to a miniature solar system. In the helium atom shown in Figure 2.1, two protons and two neutrons make up the heavy nucleus with a positive electric charge, around which two electrons with very small masses rotate. The path each electron takes around the nucleus is called an orbit. To remain in this orbit, electrons must possess a certain amount of energy, known as the electron's energy level. By virtue of their position and movement in orbit, electrons have both kinetic energy and potential energy.

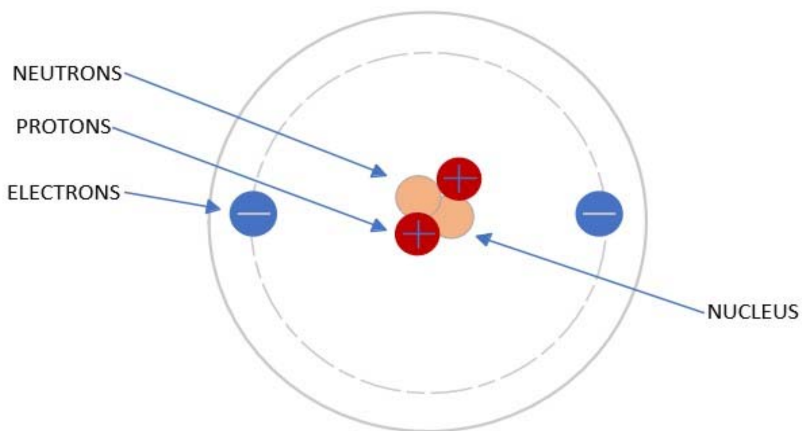


**Fig. 2.1** Helium atom

Thus, the energy possessed by an electron (kinetic and potential) is the essential factor that determines its orbital radius. For an electron to remain in orbit, it must neither gain nor lose energy. Moreover, in their orbital movement, electrons do not follow random paths but are confined to well-defined energy levels. Therefore, to move an electron from a lower energy level (closer to the nucleus) to a higher energy level, a certain amount of energy is required. This energy can come from an electric field, heat, light, or even the "bombardment" with other particles.

A consequence of the very close proximity of atoms that make up a solid material is the dissolution of the individual energy levels of the atoms and the formation of energy bands (Figure 2.2). The figure below shows the difference between the energy levels of an isolated atom and those of an atom in a solid. The isolated (gas) atom has distinct energy levels, while the atom in a solid material possesses energy bands.

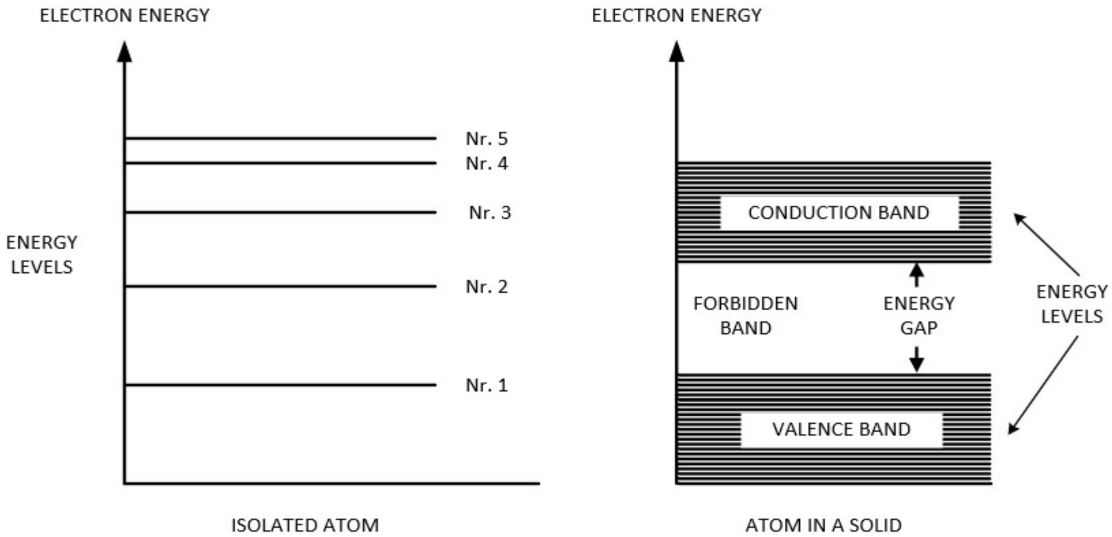


**Fig. 2.2** Energy arrangements of atoms

Electrons on the conduction band are easily removed when an external factor (electric field, light, etc.) is applied. Materials that have a large number of electrons on this band are good conductors of electricity. Below the conduction band is the forbidden band. This band will never contain electric charge carriers. Electrons only transit this sector depending on the energy input received. The last band, or the valence band, consists of a series of energy levels that contain the valence electrons. These electrons belong more to the atom itself, compared to the electrons on the conduction band. However, valence band electrons can move to the conduction band if they gain enough energy to cross the forbidden band. The thickness of the forbidden band, or the gap between the valence band and the conduction band, determines whether a material is an insulator, semiconductor, or conductor. Therefore, the materials used for producing electricity via photovoltaic cells will be semiconductors.

## 2.2 The importance of solar energy in maritime climate zones

The subject of solar energy in the maritime and coastal domain is of significant importance today. Given the growing concern for environmental conservation and the necessity to reduce carbon emissions, finding alternative energy sources is essential. This subsection of the thesis addresses the role of solar energy in maritime transport and coastal areas, highlighting the benefits that this renewable energy source brings, its integration into port infrastructure, and future implications.

### Benefits of Solar Energy in a Sustainable Maritime-Coastal Domain

Solar energy brings numerous benefits to the maritime transport industry and ports. Firstly, it significantly reduces carbon emissions and their environmental impact by replacing fossil fuel-based energy sources. This transition to cleaner energy sources plays a crucial role in combating climate change. Secondly, solar energy offers cost savings and improvements in energy efficiency. It reduces dependency on grid electricity, leading to lower operational costs. Finally, solar energy provides increased energy independence and resilience. Ports and ships equipped with solar energy systems benefit from a more reliable and stable energy source, ensuring longer operational periods.

**Integration of Solar Energy into Port Infrastructure**

Solar energy can be seamlessly integrated into various aspects of port infrastructure. Installing PV panels on rooftops and parking structures not only generates clean energy but also optimizes the use of available space. Additionally, green-powered lighting and navigation systems enhance safety and reduce energy consumption. Furthermore, using solar energy as a power source for onboard equipment on both civilian and military ships ensures a safer environment and increased comfort for the crew of these vessels.

## 3. Climate: Variability and Predictability

Global surface air temperature records from the last 150 years are characterized by a long-term warming trend with strong variability. The climate system, comprising the atmosphere, oceans, cryosphere, land surface, and its biosphere, shows variability on a multitude of time scales. Some of these time scales, such as daily and seasonal variability, are directly related to external processes to the climate system, such as variations in solar radiation[2]. These external processes are considered a pressure on the climate system, generating forced variability. However, variability also arises from internal processes within the climate system, known as internal or intrinsic climate variability. Climate variability is also caused by greenhouse gas emissions and aerosols from human activities. This variability is referred to as anthropogenic climate variability or simply climate change..

Another aspect of global warming is that many poor and marginalized communities suffer the most from extreme heat, whether due to lack of access to cooling means, being more prone to manual labor, or living in the densest and hottest parts of the world's cities. Poor countries also have the fewest resources to adapt cities, infrastructure, and food systems to be more resilient to extreme temperatures. After witnessing the impact of the hottest year on record, addressing extreme temperatures and their effects must be a priority for the near future. Cities must lead the way, whether by planting thousands of trees as in Medellin, Colombia; painting roofs white as in Ahmedabad, India; or reimagining urban planning as in Singapore. Local governments are in a position to design pragmatic solutions that can cool cities and protect the lives of over half of the world's population.[3].

### 3.1 Marine-coastal environment and its impact on pv panels

The use and implementation of renewable energy sources are rapidly gaining ground in all scenarios, with solar energy at the center of this new constellation of electricity generation technologies[4]. Solar energy can generate heat and electricity, giving rise to two technologies: solar thermal power, which collects and transforms sunlight into heat and then often into electricity; and photovoltaic (PV) technology, which directly converts sunlight into electricity.

Not only can the efficiency of installations (and therefore the price of electricity) be compromised by material defects due to environmental degradation, but reliability can also be affected. Both technologies use electronic devices, for which corrosion is a significant issue common to other sectors as well. The most common corrosion problem in PV panels is the atmospheric corrosion of the metal components of the mounting system (aluminum, steel, stainless steel, etc.). The effects of climate, atmospheric pollution, and marine spray (Fig. 3.1) cannot be ignored, as they can lead to significant degradation even after one year of exposure.

**Fig. 3.1** Salt deposits on the surface of pv panels in maritime climate[5]

Photovoltaic modules are often considered the most reliable in terms of their protection against corrosion due to encapsulation. However, corrosion remains one of the main causes of destruction of busbars, typically made of copper, aluminum, or silver; and metal contacts (molybdenum, aluminum, copper).

The complexity of corrosion mechanisms in PV cells arises from their complex structure. In cases of delamination, a confined area may appear between the layers of a PV cell that have partially or completely separated from each other. This area can trap moisture, air, and other substances, creating micro-environments where corrosion and degradation processes can accelerate. Delamination can occur due to manufacturing defects, exposure to extreme temperatures, or wear over time, affecting the performance and durability of PV modules. Understanding the mechanisms that trigger degradation kinetics helps focus on the most important factors for producing long-term stable modules and systems.

The maritime-coastal environment involves high salinity and air currents that obviously lead to salt deposits on the surface of PV panels, acting as a screen, thereby reducing the transparency and radiation flux reaching the PV cells. Studies show that this salt layer can decrease the efficiency of the PV system by up to 20-30 percent. The deposits are influenced by the humidity level of the air masses, the frequency and extent of saline spray, as well as the PV system's ability to self-clean naturally or through artificial processes. The cumulative effects of salt deposition and corrosion lead to frequent failures, resulting in additional maintenance costs. Without an adequate maintenance and protection plan for the marine environment, PV panels in coastal areas experience significant performance losses in the medium and long term.

## 4. Influence of environmental factors on a photovoltaic panel – pvsyst and labview simulation

The choice to study the effects of environmental factors on PV panels in maritime climate zones is driven by a convergence of practical, technological, and environmental considerations. The relevance and selection of this topic are underscored by several key motivations:

- Solar energy stands out as an essential component of the global transition to renewable energies. Coastal regions, with their abundant sun exposure, represent a significant opportunity for PV panel installation. However, maximizing their efficiency in these areas requires a deep understanding of how the specific environmental factors of coastal zones influence their efficiency;

- The unique environmental conditions in these coastal regions—high humidity, salt spray, strong winds, and high corrosion levels—pose significant challenges for the lifespan and performance of PV panels;
- The transition to renewable energy sources is critical for reducing the carbon footprint and combating or at least slowing down climate change, and PV panels offer a promising solution to achieve this goal. Understanding and overcoming the environmental challenges in these regions will allow for more reliable and widespread use of solar energy, contributing to a sustainable energy future;
- Advances in the resilience and efficiency of PV technology can reduce costs and improve the economic viability of projects in this vast field. This aspect is particularly important in coastal areas where harsh environmental conditions can generate higher maintenance costs and reduced efficiency;
- Coastal regions are home to a significant portion of the world's population and are often areas of intense economic activity. Improving the performance of PV systems in these areas can have widespread benefits, from local energy independence to global environmental benefits by reducing the carbon footprint.

Studying the effects of environmental factors on PV panels operating in the maritime-coastal environment is not just a technical challenge, but also an important step toward achieving larger sustainability goals.

### 4.1 The Shockley mathematical model

This software utilizes detailed mathematical models to simulate the efficiency and performance of photovoltaic systems. In this subsection, the Shockley mathematical model is presented[6], which is used by the software to carry out the simulation.

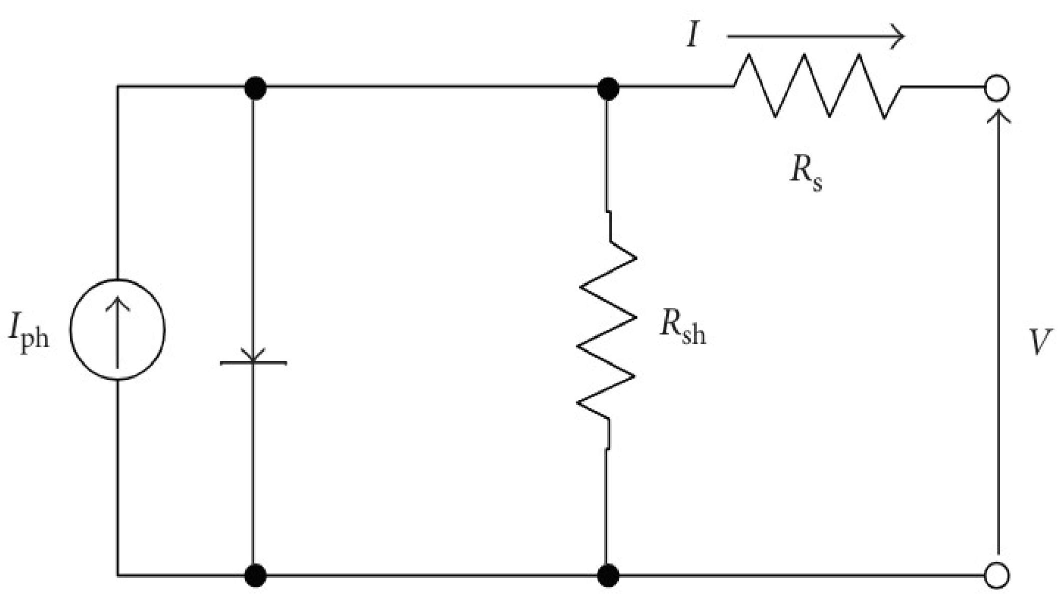


**Fig. 4.1** Equivalent circuit diagram (with a single diode) used by pvsyst software [7]

At a given illumination, the current-voltage relationship is given by (4.1):

$$I = I_{ph} - I_0 \cdot \left[ e^{\frac{q \cdot (V + I \cdot R_S)}{N_{CS} \cdot \gamma \cdot K_B \cdot T}} - 1 \right] - \frac{V + I \cdot R_S}{R_{sh}} \quad (4.1)$$

where:
I - current generated by the module [A];
V - voltage at the module terminals [V];
Iph - photocurrent [A], proportional to irradiation G, with a correction based on T;
I0 - reverse saturation current, temperature dependent [A];
Rs - series resistance [ohm];
Rsh - shunt resistance [ohm];
q - charge of the electron - 1.602·E-19 Coulomb;
KB - Boltzmann constant - 1.381 E-23 J/K;
γ - diode quality factor, usually between 1 and 2;
Ncs - number of cells in series;
T - effective temperature of the cells [K].

The parameters in equation (4.1) correspond to the intrinsic characteristics of the construction of a solar cell. The series resistance $R_s$ represents the total resistance of the cell and is a combination of all its internal resistances. The shunt resistance $R_{sh}$, represents the alternative paths through which current can deviate from the PN junction, leading to current losses.

Decreasing the series resistance $R_s$ will lead to an increase in the short-circuit current and maximum voltage, while increasing the shunt resistance $R_{sh}$ causes the open-circuit voltage and maximum current to rise[8].

### 4.2. Influence of environmental factors – pvsyst simulation

**Table 4.1 Location Parameters**

| Country | Romania |
|---|---|
| City | Constanța |
| Location | "Mircea cel Bătrân" Naval Academy |
| Latitude | 44.18° N |
| Longitude | 28.61° E |
| Altitude | 71 m |
| Weather Data | Meteonorm 8.1 (PVsyst) |

Geographical site parameters, new site

Geographical Coordinates | Monthly meteo | Interactive Map

Site **I.C. Brătianu (Romania)**

Data source Meteonorm 8.1 (1991-2006)

| | Global horizontal irradiation | Horizontal diffuse irradiation | Temperature | Wind Velocity | Linke turbidity | Relative humidity |
|---|---|---|---|---|---|---|
| | kWh/m²/mth | kWh/m²/mth | °C | m/s | [-] | % |
| January | 43.5 | 24.0 | 0.8 | 3.70 | 3.012 | 83.1 |
| February | 68.9 | 33.7 | 2.2 | 3.60 | 3.359 | 82.3 |
| March | 101.0 | 54.9 | 6.3 | 3.50 | 3.738 | 74.9 |
| April | 144.1 | 70.2 | 10.7 | 3.10 | 4.310 | 73.9 |
| May | 190.1 | 86.0 | 16.8 | 2.90 | 3.790 | 72.7 |
| June | 211.5 | 80.6 | 21.2 | 2.81 | 3.606 | 70.4 |
| July | 213.3 | 75.8 | 24.0 | 2.69 | 3.632 | 65.7 |
| August | 180.3 | 69.9 | 24.1 | 2.69 | 3.691 | 65.6 |
| September | 132.6 | 48.9 | 18.8 | 3.00 | 3.606 | 70.8 |
| October | 85.1 | 42.1 | 13.2 | 3.10 | 3.372 | 78.1 |
| November | 47.2 | 27.4 | 8.4 | 3.10 | 3.203 | 83.2 |
| December | 37.3 | 23.7 | 3.0 | 3.49 | 3.048 | 82.2 |
| **Year** | **1454.9** | **637.3** | **12.4** | **3.1** | **3.531** | **75.2** |

**Global horizontal irradiation year-to-year variability 4.7%**

**Fig. 4.2** Meteorological data table - pvsyst for the selected location[9]

**PV Array Characteristics**

| PV module | | Inverter | |
|---|---|---|---|
| Manufacturer | CSI Solar | Manufacturer | Generic |
| Model | CS6A - 230MS | Model | 3 kWac inverter |
| (Original PVsyst database) | | (Original PVsyst database) | |
| Unit Nom. Power | 230 Wp | Unit Nom. Power | 3.00 kWac |
| Number of PV modules | 84 units | Number of inverters | 6 units |
| Nominal (STC) | 19.32 kWp | Total power | 18.0 kWac |
| Modules | 6 Strings x 14 In series | Operating voltage | 125-440 V |
| **At operating cond. (50°C)** | | Pnom ratio (DC:AC) | 1.07 |
| Pmpp | 17.43 kWp | | |
| U mpp | 320 V | | |
| I mpp | 54 A | | |
| **Total PV power** | | **Total inverter power** | |
| Nominal (STC) | 19 kWp | Total power | 18 kWac |
| Total | 84 modules | Number of inverters | 6 units |
| Module area | 109 m² | Pnom ratio | 1.07 |
| Cell area | 98.5 m² | | |

**Fig. 4.3** PV array charateristics

The photovoltaic module used for the simulation is a CSI Solar module. It consists of 6 strings, each with 14 modules in series, with an inclination angle of 45° and a total area of 109 m².

For this module, the following data resulting from the simulations were analyzed: the module's Performance Ratio (PR), the maximum virtual energy generated, and the losses due to temperature.

The Performance Ratio (PR) indicates the efficiency of the PV collector without considering the effect of external parameters. It is defined as the ratio between the measured produced power and the nominal power determined from the electrical characteristics of the cell or collector under Standard Test Conditions (STC)[10].

The PR equation can be written as follows[10]:

$$PR = \frac{P_{mas}}{P_m} \cdot \frac{G}{1000} \tag{4.2}$$

where $P_m$ is the power developed by the PV collector at the maximum operating point, and $P_{mas}$ is the power developed by the collector at the solar irradiance intensity $G$.

The final results of the simulation were selected from the report generated by PVsyst and were chosen to clearly highlight the amount of solar energy captured and converted into electrical energy, as well as the losses encountered based on the analyzed parameters.

The data analyzed for the study of the three environmental factors referred to in this subsection were obtained through repeated simulations using the free version 7.3.1 of the PVsyst software. In the first standard simulation, the preset parameter values from the program's database were used, and the values obtained are shown in the following table:

**Table nr. 4.2 Simulation results**

| Parameter | Average wind value [m/s] | | | Average temperature value [°C] | | | Average humidity value [%] | | |
|---|---|---|---|---|---|---|---|---|---|
| | 3.1 | 13.1 | 18.1 | 12.4 | 22.4 | 27.4 | 75.2 | 37.6 | 0 |
| Performance ratio PR [%] | 86 | 86.73 | 86.73 | 86 | 82.93 | 81.01 | 86 | 86.73 | 86.73 |
| Array virtual energy [kWh] | 28.103 | 28.894 | 28.894 | 28.103 | 27.633 | 26.995 | 28.103 | 28.894 | 28.894 |
| PV loss due to temperature [%] | 6.71 | 6.08 | 6.08 | 6.71 | 10.14 | 12.19 | 6.71 | 6.08 | 6.08 |

The largest differences in the analyzed results, presented in Table 4.2, were obtained with variations in ambient temperature[11], [12], [13]. Improvements in the efficiency of the photovoltaic panel system were also observed with increases in wind speed and decreases in air humidity. It is certain that, on a macro level, modifying these parameters is impossible; however, there are improvements in this regard in the naval field because systems operated in this environment benefit from much better cooling due to the presence of marine air currents, which are cooler and more frequent than coastal currents.

The combination of various variations for the three influencing factors is random in real situations. From this perspective, only simulation can draw conclusions. Real situations cause operation to occur with a random combination of factors. With more advanced methods of randomly combining the levels of influencing factors, these situations can also be investigated, but the information gain is minimal.

### 4.3 Influence of environmental factors/mathematical model

Therefore, the equation (4.1) presented earlier in this chapter is derived from equation (4.8), by introducing the series and shunt resistances present in a PV cell.

To simulate the behavior of a photovoltaic cell under variations in wind and ambient temperature using LabView software, a mathematical model is necessary. The specialized literature proposes several studies regarding the action and manner in which the wind cools the surface of PV cells, thus improving their efficiency[14][15], [16], [17], [18]. For this, an equation is needed that encompasses both the temperature of the PV cell and the wind that influences this temperature.

Therefore, according to C. Schwingshackl et al[14], the temperature of a cell is calculated as follows:

$$T_c = T_a + \frac{G}{G_{NOCT}} \cdot (T_{NOCT} - T_{aNOCT}) \qquad (4.3)$$

where:

$T_c$ – is the temperature of the cell [K];
$T_a$ – is the ambient temperature [K];
$G$ – is the irradiance on the plane of the PV panel [W/m$^2$];
$G_{NOCT}$ – is the irradiance at the nominal operating cell temperature [W/m$^2$];
$T_{NOCT}$ – is the nominal operating cell temperature (318.15 K, approximately 45[°C]);
$T_{aNOCT}$ – is the ambient temperature at standard operating conditions - ($T_{aNOCT}$ = 20[°C]);
**$G_{NOCT}$ = 800 [W/m$^2$];**
**$T_{NOCT}$ = 318,15 [K];**
**$T_{aNOCT}$ = 293,15 [K].**
$NOCT$ – Normal Operating Cell Temperature (Temperatura Nominală de Operare a Celulei)

Skoplaki et al. suggest an advanced model to integrate wind into the standard NOCT formula (equation 4.4). This model considers, in addition to the ambient temperature $T_a$ and the irradiance $G$ reaching the PV cell, the wind speed $v$ and specific properties of PV cells, such as efficiency η, temperature coefficient of maximum power β, transmittance of the covering system τ and absorption coefficient of the PV cells, α.

Thus, equation (4.4) becomes:

$$T_c = T_a + \frac{G}{G_{NOCT}} \cdot (T_{NOCT} - T_{aNOCT}) \cdot \frac{h_{wNOCT}}{h_w(v)} \cdot \left[1 - \frac{\eta_{STC}}{\tau \cdot \alpha}(1 - \beta_{STC} T_{STC})\right] \qquad (4.4)$$

where:

- $\eta_{STC}$ and $\beta_{STC}$ are the efficiency and temperature coefficient of maximum power under standard test conditions (STC): irradiance of 1000 W/m², ambient temperature of 25°C, and air mass 1.5. The values for efficiency and the temperature coefficient of maximum power are listed in Table 4.7 above. The value for τ·α can usually be assumed to be 0.9.

- $h_{wNOCT}$ – wind convection coefficient for wind speed under NOCT conditions;
$v_w$ ($NOCT$) = 1 m/s;

- $h_w$ – The wind convection coefficient. This parameter is a linear function of wind speed and presents two different values depending on the location where the climatic factor being analyzed is measured:

$$h_w = 8.91 + 2 \cdot v_f \tag{4.5}$$

$$h_w = 5.7 + 2.8 \cdot v_w \tag{4.6}$$

where:

$v_f$ – Wind speed measured at 10 meters above the PV panel;
$v_w$ – Wind speed near the PV panel;

Two other equations for the wind convection coefficient are presented below[15], [19]:

$$h_w = 8.3 + 2.2 \cdot v_w, \ h_{wNOCT} = 10.5 \tag{4.7}$$

- for wind directions perpendicular to the surface of the PV panel;

$$h_w = 6.5 + 3.3 \cdot v_w, \ h_{wNOCT} = 9.8 \tag{4.8}$$

- for wind directions parallel to the surface of the PV module

To create the equation of the mathematical model that will be implemented in the LabVIEW programming software, I will start from equation (4.1) which describes the current generated by a PV cell. According to the specialized literature, the formula for the photocurrent is as follows:

$$I_{ph} = \frac{G}{G_{ref}} \cdot \left[I_{phref} + \mu_{ISC} \cdot \left(T - T_{ref}\right)\right] \tag{4.9}$$

where:

$G_{ref}$ – reference irradiance (1000) [W/m²];
$T_{ref}$ – reference temperature of the cell [K] (298.15 K or 25°C);
$\mu_{ISC}$ = temperature coefficient of the photocurrent (+0.05%/°C).

In the current equation (4.1), we substitute equation (4.4) and obtain:

$$I = I_{ph} - I_0 \cdot \left[ e^{\left( \frac{q(V+IR_S)}{N_{CS} \cdot \gamma \cdot K_B \cdot \left(T_a + \frac{G}{G_{NOCT}} \cdot (T_{NOCT} - T_{aNOCT}) \cdot \frac{h_{wNOCT}}{h_w(v)} \cdot \left[1 - \frac{\eta_{STC}}{\tau \cdot \alpha}(1 - \beta_{STC} T_{STC})\right]\right)} \right)} - 1 \right] - \frac{V + I \cdot R_S}{R_{SH}} \tag{4.10}$$

$R_s$ – series resistance = 1398 [Ω];

$R_{sh}$ - shunt resistance = 1000 [Ω];

$I_0$ – reverse saturation current = 4.12 x $10^{-10}$ [A]; all these parameters are provided by the manufacturer of the PV panel used for the simulation (10 Wp), which will be described in the next chapter.

This last equation incorporates temperature and wind dependence, showing the complex influence of environmental conditions on the current generated by a PV cell. It highlights how environmental factors such as wind speed and ambient temperature affect the cell's operation and consequently its efficiency.

### 4.4 Simulation in LabVIEW of a pv panel with a maximum power of 10 wp

Following the simulations, we initially analyzed the influence of ambient temperature on the current produced by a PV cell.

From the data presented in Table 4.3 below, a consistent increase in current as the temperature rises can be observed. This behavior is well-known in the PV energy field because the performance characteristics of the semiconductor materials used in PV cell construction degrade as temperatures increase.

The current increases from 0.60210 A at 25°C to 0.60996 A at 50°C. This confirms that high temperatures influence the generation of charge carriers, and when combined with their high mobility, this results in an increase in short-circuit current but a significant reduction in the voltage produced by the cell. The drop in produced voltage more strongly affects the total generated power. Therefore, despite a slight increase in the produced current, the larger decrease in voltage will lead to an overall reduction in efficiency and total power developed by the PV cell at high temperatures[20], [21].

After calculating the average rate of current increase per degree Celsius, it is found that, on average, the generated current increases by approximately 0.0003144 A for each additional degree Celsius. The graph in Fig. 4.4 clearly illustrates how the current value rises as the temperature increases.

**Table 4.3 Current values obtained at various temperature changes**

| Nr. crt. | Temperature (°C) | Current (A) | Wind speed (m/s) |
|---|---|---|---|
| 1. | 25 | 0,60210 | 0 |
| 2. | 26 | 0,60242 | 0 |
| 3. | 27 | 0,60273 | 0 |
| 4. | 28 | 0,60305 | 0 |
| 5. | 29 | 0,60336 | 0 |
| 6. | 30 | 0,60368 | 0 |
| 7. | 31 | 0,60399 | 0 |
| 8. | 32 | 0,60399 | 0 |
| 9. | 33 | 0,60462 | 0 |
| 10. | 34 | 0,60494 | 0 |
| 11. | 35 | 0,60525 | 0 |
| 12. | 36 | 0,60557 | 0 |
| 13. | 37 | 0,60588 | 0 |
| 14. | 38 | 0,60620 | 0 |
| 15. | 39 | 0,60651 | 0 |
| 16. | 40 | 0,60683 | 0 |
| 17. | 41 | 0,60714 | 0 |
| 18. | 42 | 0,60746 | 0 |
| 19. | 43 | 0,60777 | 0 |
| 20. | 44 | 0,60809 | 0 |
| 21. | 45 | 0,60840 | 0 |
| 22. | 46 | 0,60872 | 0 |
| 23. | 47 | 0,60903 | 0 |
| 24. | 48 | 0,60935 | 0 |
| 25. | 49 | 0,60966 | 0 |
| 26. | 50 | 0,60996 | 0 |

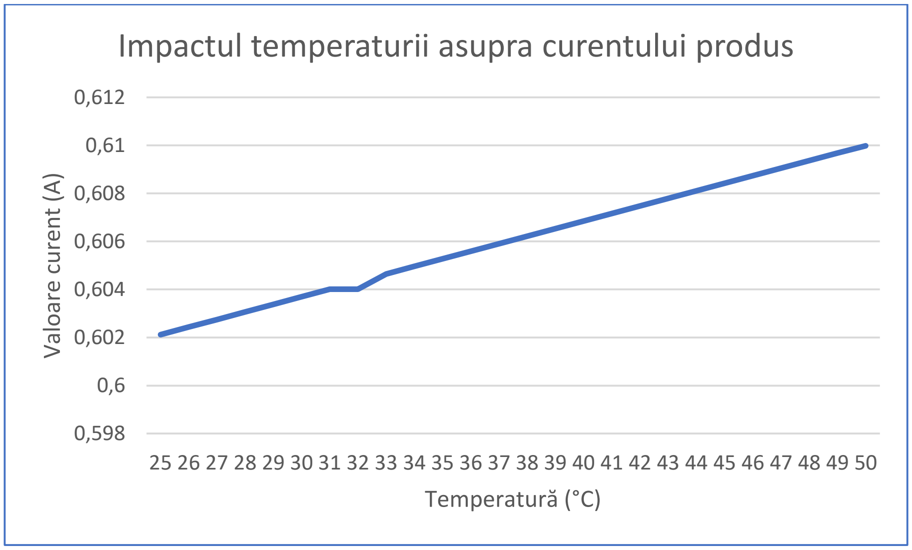


**Fig. 4.4** Variation of produced current

In the second stage, we analyzed the variation of the produced current considering the effect of wind speed on the PV cell. We kept the ambient temperature constant at 50°C and gradually increased the wind speed from 0 to 25 m/s, as shown in the table below.

**Table 4.4 Current values obtained at various wind speeds**

| Nr. crt. | Wind speed (m/s) | Current (A) | Temperature (°C) |
|---|---|---|---|
| 1. | 0 | 0,60996 | 50 |
| 2. | 1 | 0,61011 | 50 |
| 3. | 2 | 0,61026 | 50 |
| 4. | 3 | 0,61041 | 50 |
| 5. | 4 | 0,61056 | 50 |
| 6. | 5 | 0,61071 | 50 |
| 7. | 6 | 0,61086 | 50 |
| 8. | 7 | 0,61101 | 50 |
| 9. | 8 | 0,61116 | 50 |
| 10. | 9 | 0,61131 | 50 |
| 11. | 10 | 0,61146 | 50 |
| 12. | 11 | 0,61161 | 50 |
| 13. | 12 | 0,61176 | 50 |
| 14. | 13 | 0,61191 | 50 |
| 15. | 14 | 0,61206 | 50 |
| 16. | 15 | 0,61221 | 50 |
| 17. | 16 | 0,61236 | 50 |
| 18. | 17 | 0,61251 | 50 |
| 19. | 18 | 0,61266 | 50 |
| 20. | 19 | 0,61281 | 50 |
| 21. | 20 | 0,61296 | 50 |
| 22. | 21 | 0,61311 | 50 |
| 23. | 22 | 0,61326 | 50 |
| 24. | 23 | 0,61341 | 50 |
| 25. | 24 | 0,61356 | 50 |
| 26. | 25 | 0,61371 | 50 |

As expected, we observed that wind speed has a positive effect on the efficiency of a PV cell. When the wind speed increases, the value of the current produced by the cell also increases. Wind speed helps cool the PV panel, which leads to an increase in efficiency.

According to Table 4.4, the current increases steadily from 0.60996 A at a wind speed of 0 m/s to 0.61371 A at a wind speed of 25 m/s. To quantify the impact of wind on the produced current, we calculated the average rate of increase for each variation in wind speed. We found that, on average, the current increases by approximately 0.0001248 A for every 1 m/s increase in wind speed. This confirms the positive influence of wind in the context of photovoltaic energy.

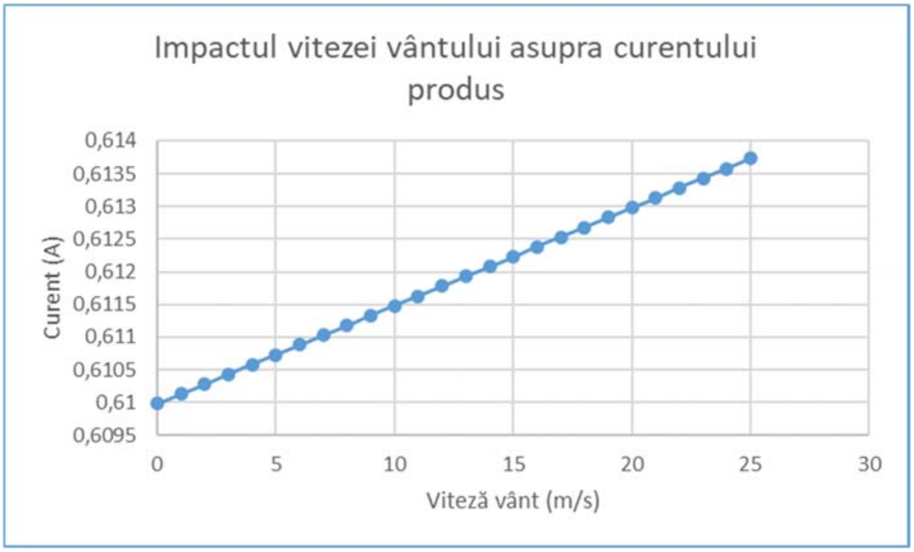


**Fig. 4.5** Variation of produced current

In the third and final stage of this subsection, we analyzed the combined impact of ambient temperature and wind speed on the efficiency of a PV cell. Combinations of low temperatures (25-30°C) and low wind speeds (0-5 m/s) show the lowest values of produced current.

As expected, combinations of high temperatures (45-50°C) and high wind speeds (15-25 m/s) show the highest values of produced current. This confirms once again that high temperatures increase the current value but reduce the efficiency of the PV cell by decreasing the open-circuit voltage, resulting in lower overall cell efficiency.

Comparing the rate of current increase based only on temperature, without considering the cooling effect of wind from the first stage (0.0003144 A/°C) with the combined rate of increase obtained in the final stage of the simulation (0.00048 A/°C), a higher rate of increase is observed.

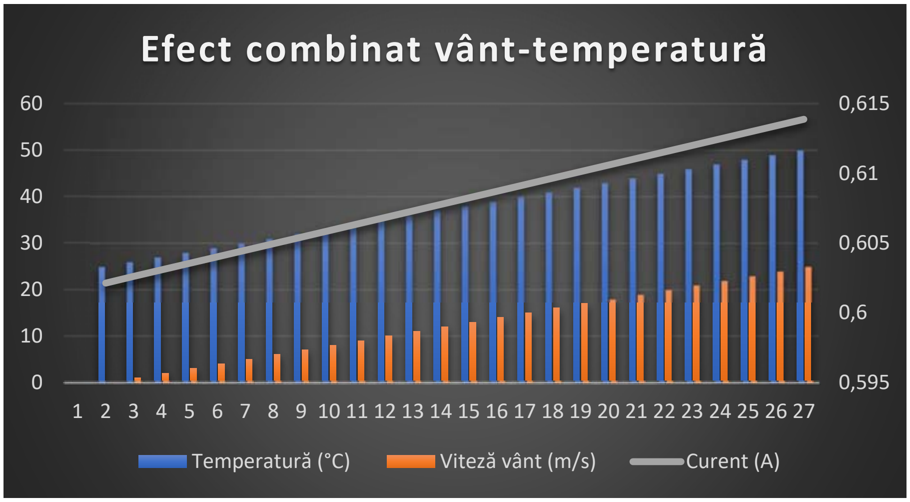


**Fig. 4.6** Variation of produced current

**Table 4.5 Current values obtained with combined wind-temperature effect**

| Nr. crt. | Temperature (°C) | Wind speed (m/s) | Current (A) |
|---|---|---|---|
| 1. | 25 | 0 | 0,60210 |
| 2. | 26 | 1 | 0,60257 |
| 3. | 27 | 2 | 0,60304 |
| 4. | 28 | 3 | 0,60351 |
| 5. | 29 | 4 | 0,60398 |
| 6. | 30 | 5 | 0,60445 |
| 7. | 31 | 6 | 0,60492 |
| 8. | 32 | 7 | 0,60539 |
| 9. | 33 | 8 | 0,60586 |
| 10. | 34 | 9 | 0,60633 |
| 11. | 35 | 10 | 0,60680 |
| 12. | 36 | 11 | 0,60727 |
| 13. | 37 | 12 | 0,60774 |
| 14. | 38 | 13 | 0,60821 |
| 15. | 39 | 14 | 0,60868 |
| 16. | 40 | 15 | 0,60915 |
| 17. | 41 | 16 | 0,60962 |
| 18. | 42 | 17 | 0,61009 |
| 19. | 43 | 18 | 0,61056 |
| 20. | 44 | 19 | 0,61103 |
| 21. | 45 | 20 | 0,61150 |
| 22. | 46 | 21 | 0,61197 |
| 23. | 47 | 22 | 0,61244 |
| 24. | 48 | 23 | 0,61291 |
| 25. | 49 | 24 | 0,61338 |
| 26. | 50 | 25 | 0,61371 |

Analyzing the values obtained from the two simulations with different software confirms that ambient temperature has a negative effect on the efficiency of the PV cell. The average rate of current increase per degree Celsius observed in the simulations indicates an increased sensitivity of PV panel performance to temperature variations. Therefore, in areas with high temperatures, it is necessary to implement cooling strategies (passive or active) to maintain PV systems operating within optimal parameters. Similarly, the simulations show how wind speed positively influences the efficiency of the cells. Faster movements of air masses near the PV panels cool them, and the value of the produced current increases.

Ideal locations for installing PV systems should have moderate temperatures and constant winds, ensuring efficient cooling. Regarding construction, PV systems should be designed with artificial cooling solutions, monitoring systems for wind speed and ambient temperature, and self-cleaning capabilities as much as possible, especially for installations in isolated areas.

## 5. Description of the experimental stand

**Table 5.1 Characteristics of the pv panel used in the simulation**

| Parameter | Value |
|---|---|
| Maximum Power ($P_{max}$) | 10 W |
| Maximum Current ($I_{mp}$) | 0.55 A |
| Voltage at $P_{max}$ ($V_{mp}$) | 18 V |
| Short-Circuit Current ($I_{sc}$) | 0.62 A |
| Open-Circuit Voltage ($V_{oc}$) | 21.49 V |
| Dimensions | 300x280x17 mm |

**Fig. 5.1** Used PV panel

The data acquisition stand configuration includes a 10 Wp PV panel, a load, and a data acquisition system. The data collection was carried out by mounting the PV panel on the building of the Faculty of Marine Engineering at the "Mircea cel Bătrân" Naval Academy.

The data acquisition was performed using the USB-6008 multifunction module. This product features two single-ended analog input channels[22] (in this configuration, each input channel has one wire connected to the signal source and another wire connected to the ground), as well as 12 digital input/output channels with a total of 32 bits. We used a single analog input to record the voltage produced by the PV panel and a ground input.

With one or more channels, the National Instruments USB-6008 multifunction device can measure and record the analog signal 10,000 times per second, ensuring accurate data capture. It is equipped with a USB connection, an LED, and two screw terminal connectors. The USB connection is for a high-speed USB interface, while the screw terminal connectors are for data acquisition from sensors and control signal transmission (input/output). The green LED lights up to indicate the device's status. Single-ended analog readings can be obtained from the 8 analog inputs or differential readings from 4 of them. The USB-6008 module includes an analog-to-digital converter for converting analog signals to digital signals and a programmable gain amplifier for adjusting the input gains when the instrument is configured for differential measurements.


**Fig. 5.2** USB 6008 Module – National Instruments[23]

**5.1 Data acquisition and analysis for a 10 Wp PV panel**

The PV panel was installed on the building of the Faculty of Marine Engineering at the "Mircea cel Bătrân" Naval Academy, with an inclination of 45 degrees. The data acquisition period was 13 weeks (26.02-26.05.2024). Meteorological data (wind speed, gust wind speed, ambient temperature, and humidity) were provided by the Maritime Hydrographic Directorate "Commander Alexandru Cătuneanu" – Constanța.

**Fig. 5.3** Installation of the PV panel on the building of the Faculty of Marine Engineering

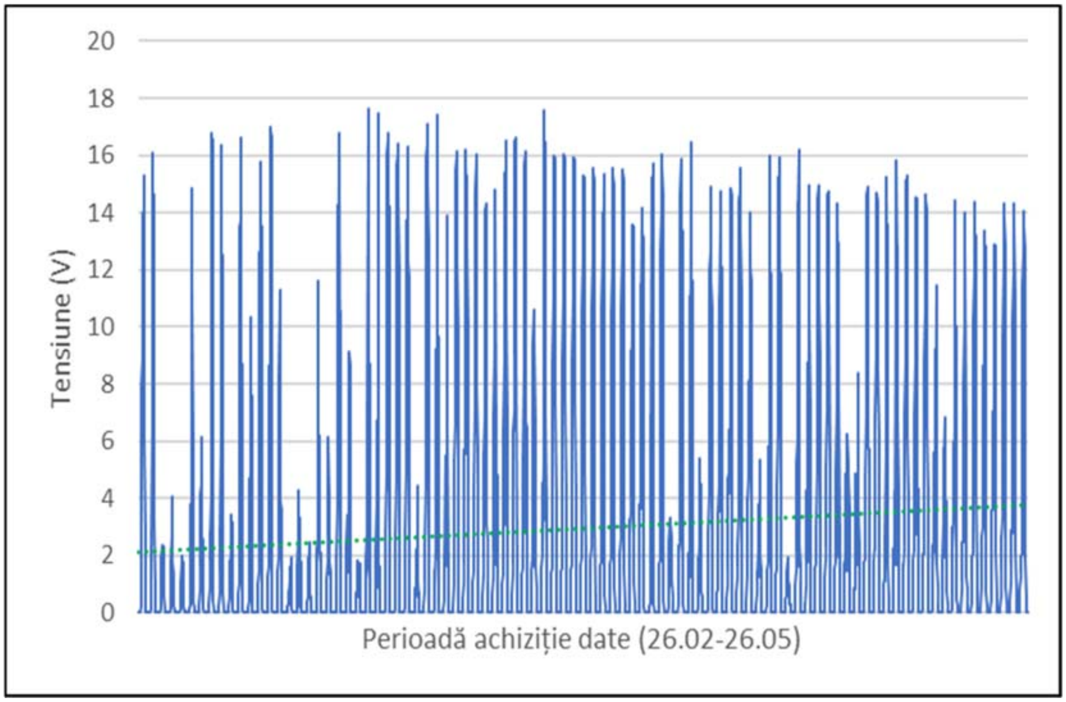


**Fig. 5.4** Voltage production of the 10 Wp PV panel

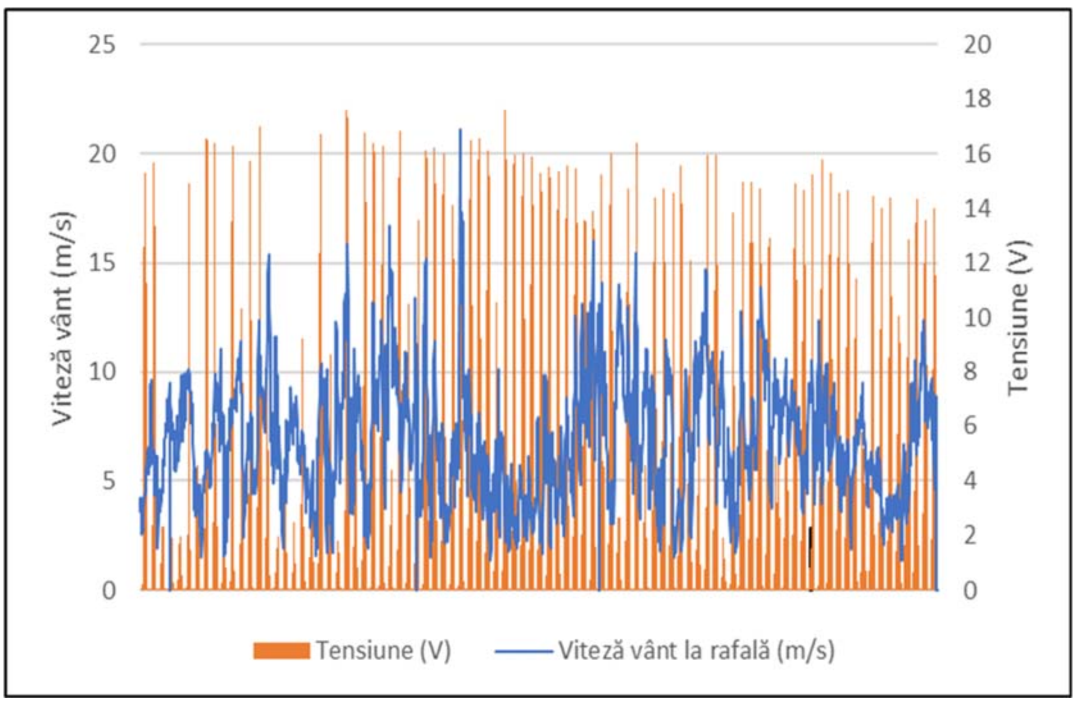


**Fig. 5.5** Voltage-Wind dependence for the period 26.02-26.05.2024

**Figure 5.4** shows the voltage values produced by the PV panel in the experimental setup. The time interval covers approximately three months, and the voltage exhibits significant variability over the analyzed period, with many spikes. This is mainly due to day/night alternations and changes in meteorological factors that directly influence the efficiency of the PV panel. The dotted green line represents the general trend of the voltage, which remains almost constant around 2-3 V.

**Figure 5.5** illustrates the dependence between the voltage produced by the coastal PV panel and the gust wind speed for the entire data acquisition period. Both wind speed and voltage show significant variations and oscillatory behavior over the analyzed time interval. In terms of the relationship between wind speed and produced voltage, we observe a positive correlation; when wind speed increases, the produced voltage tends to increase as well. However, the voltage peaks do not always correspond to the wind speed peaks, suggesting the presence of other factors influencing the system's performance.

The fluctuations in wind speed are relatively evenly distributed over the analyzed period, with values ranging between 0 and 23 m/s. These rapid variations in wind intensity are reflected in the produced voltage values, which range between 0 and 18 V. This variability suggests that the PV panel is sensitive to rapid changes in meteorological factors, in this case, wind speed.

The observed dependence between wind speed and the voltage produced by the PV panel is a crucial process for optimizing the performance of PV systems for electricity generation. Thus, we can implement measures to maximize production during periods of strong wind or mitigate sudden voltage variations for a consistent supply to the electrical grid.

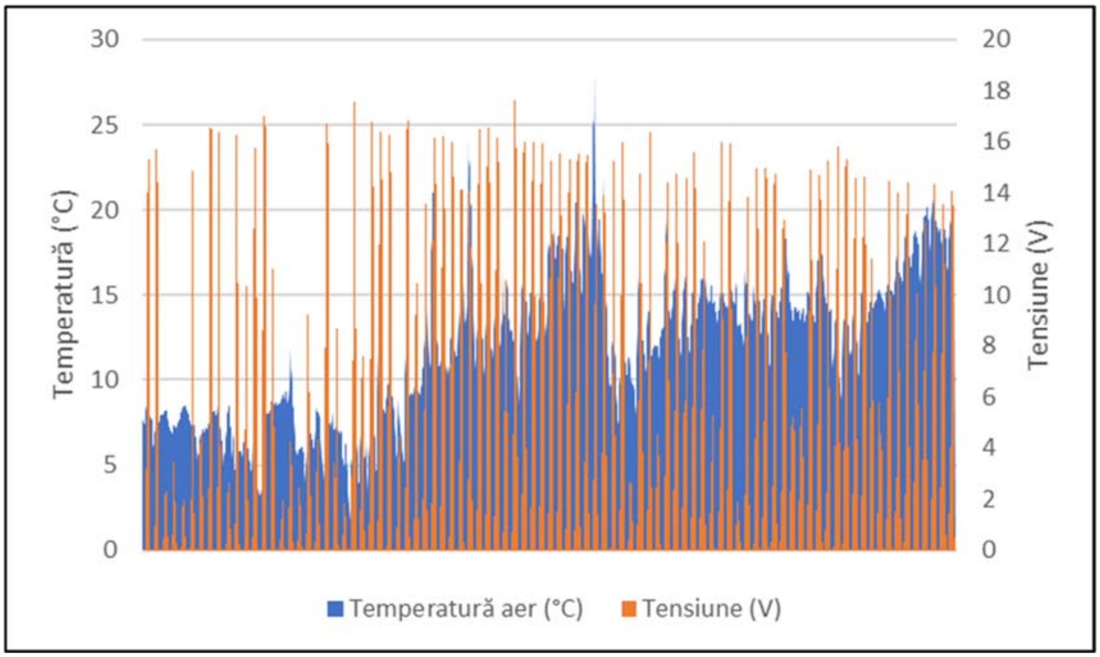


**Fig. 5.6** Voltage-Temperature dependence for the period 26.02-26.05.2024

The graph above indicates the relationship between the ambient air temperature measured in °C and the voltage produced by the experimental setup for the same period. The temperature data are represented by the blue line, while the voltage data are represented by the orange line. This graph allows us to observe how air temperature influences the performance of the PV panel.

The air temperature fluctuates significantly, ranging between 0°C and 29°C. These variations are due to day-night and seasonal alternations, with temperature increases indicating daily heating and cooling cycles. Typically, temperatures rise during the day, peaking in the afternoon, and fall at night, aligning with natural weather patterns.

The produced voltage also shows considerable variability, oscillating between 0 V and 18 V. The relationship between temperature and the efficiency of a PV panel is not straightforward. Contrary to what might initially be assumed, an increase in temperature often leads to a decrease in the voltage produced by the PV system. The graph shows instances where higher temperatures correspond to lower voltage levels, highlighting the inhibitory effect of temperature on PV efficiency. Conversely, during cooler periods, the voltage tends to be higher, demonstrating the improved performance of PV cells at lower temperatures.

The analysis of the graphs presented above illustrates the performance of PV systems under variable meteorological conditions and provides important insights into how these systems behave in real-world scenarios. The findings confirm the results obtained through simulations in Chapter 4 of this thesis, thereby enhancing the understanding of the environmental factors influencing PV efficiency.

## 5.2 Influence of air humidity on the efficiency of the experimental stand

**Fig. 5.7** Execution of the experiment and measurement process

After conducting the measurements, I proceeded to compile a table with the recorded data.

This time, we analyzed the voltage produced by the PV panel in relation to artificially created humidity, and the obtained values are presented in the following table.

**Tablenr. 5.2 Voltage values obtained at different humidity levels**

| Nr. crt. | Relative Humidity (%) | Voltage (V) | Current (A) |
|---|---|---|---|
| 1. | 22 | 16,39 | 0,546 |
| 2. | 23 | 16,32 | 0,544 |
| 3. | 24 | 16,25 | 0,542 |
| 4. | 25 | 16,63 | 0,554 |
| 5. | 32 | 14,36 | 0,479 |
| 6. | 33 | 14,29 | 0,476 |
| 7. | 34 | 14,26 | 0,475 |
| 8. | 35 | 14,31 | 0,477 |
| 9. | 36 | 14,16 | 0,472 |

| | | | |
|---|---|---|---|
| 10. | 37 | 14,88 | 0,496 |
| 11. | 38 | 14,93 | 0,498 |
| 12. | 39 | 14,30 | 0,477 |
| 13. | 41 | 14,44 | 0,481 |
| 14. | 40 | 14,31 | 0,477 |
| 15. | 42 | 14,25 | 0,475 |
| 16. | 43 | 14,20 | 0,473 |
| 17. | 44 | 14,08 | 0,469 |
| 18. | 46 | 13,66 | 0,455 |
| 19. | 47 | 13,51 | 0,450 |
| 20. | 48 | 14,22 | 0,474 |
| 21. | 49 | 13,59 | 0,453 |
| 22. | 50 | 13,50 | 0,450 |
| 23. | 51 | 13,49 | 0,450 |
| 24. | 52 | 13,48 | 0,449 |
| 25. | 54 | 13,45 | 0,448 |
| 26. | 55 | 13,40 | 0,447 |
| 27. | 56 | 13,47 | 0,449 |

The presented data indicate a relationship between the two analyzed parameters. It is observed that as humidity increases, the voltage tends to decrease. This result was anticipated in Chapter 4 of this thesis, during the PVsyst simulation.

Analyzing the recorded humidity values, we observed a gradual increase from 22% to 56% (the maximum we were able to achieve in the experiment). This variation is not linear but shows a clear increasing trend over the observation period.

The voltage values start at 16.39 V for the lowest humidity value (22%) and gradually decrease to 13.47 V for the highest humidity value (56%), indicating a general decline, with some intermediate fluctuations.

This inverse relationship between humidity and voltage can be explained by several physical mechanisms. Increased humidity can affect the electrical characteristics of the PV panel (insulation resistance of materials – creating additional losses in the circuit). It is certain that humidity affects the transmission of light to the photovoltaic cells through the accumulation of condensation or by altering the optical properties of the light-absorbing surface of the panel. The figure below indicates the inverse relationship between humidity and the efficiency of the PV panel.

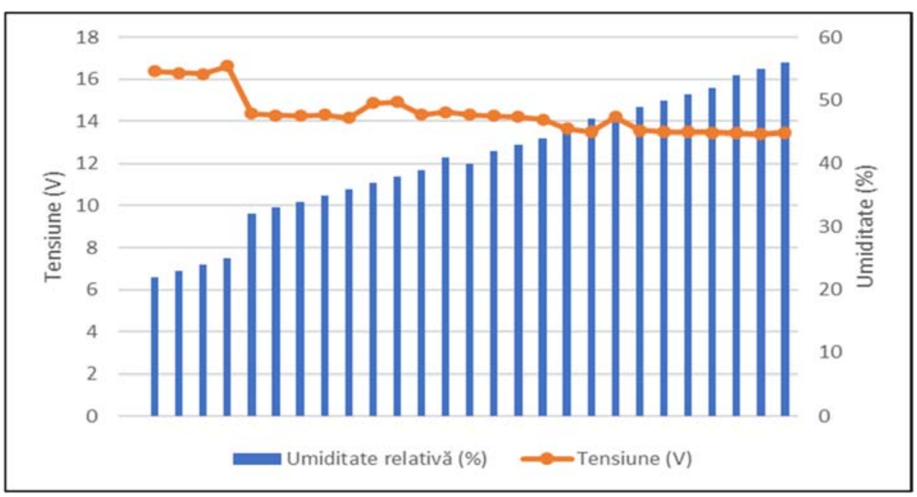


**Fig. 5.8** The inverse relationship between humidity and voltage

The simulations accurately predicted the behavior of PV panels under varying environmental conditions (in this case – marine climate zones), and the experimental data confirmed these predictions. Specifically, we observed how increasing temperature generally leads to a decrease in PV panel efficiency. This can be attributed to the intrinsic characteristics of the semiconductor materials used in the construction of the panels, which exhibit lower efficiency at higher operating temperatures, leading to the recombination of electron-hole pairs.

I also found that humidity affects the efficiency of the panels in the same way as temperature. As humidity levels increase, there is a notable decrease in the voltage produced by the PV panel on which we conducted the experiment.

Wind speed, although not as impactful as temperature and humidity, plays a very important role in positively influencing the efficiency of the PV panel used in the experiment. Wind speed helps cool the panels, partially mitigating the negative effects of high temperatures. However, extreme wind conditions can physically damage PV systems or lead to the accumulation of dirt on the light-absorbing surface of the panels, especially in marine climate zones where salt spray and sand particles are present.

The successful alignment of simulation and experimental data emphasizes the robustness of the mathematical models used in this thesis. This confirms that the mathematical models can reliably predict the performance of PV panels across a wide range of environmental conditions. This alignment also validates the experimental setup and methodology, affirming that the stand accurately reflects real conditions.

Therefore, the conclusions drawn from this chapter highlight the critical need to consider environmental factors in the design and implementation of PV systems. By understanding and anticipating the impact of ambient temperature, wind speed, and humidity, it is possible to optimize the placement and maintenance of PV panels to maximize their efficiency and longevity. This research provides valuable insights that can support future advancements in PV technology and the operational practices of renewable energy sources.

## BIBLIOGRAFIE

[1] "Riviera - News Content Hub - Eco Marine Power receives AiP for renewable energy system." Accessed: Apr. 14, 2024. [Online]. Available: https://www.rivieramm.com/news-content-hub/news-content-hub/eco-marine-power-receives-aip-for-marine-renewable-energy-system-65724

[2] G. C. Hegerl *et al.*, "Causes of climate change over the historical record," Dec. 09, 2019, *Institute of Physics Publishing*. doi: 10.1088/1748-9326/ab4557.

[3] "4 Climate Stories that Will Define 2024 | World Resources Institute." Accessed: Jun. 11, 2024. [Online]. Available: https://www.wri.org/insights/4-climate-stories-will-define-2024

[4] "World Energy Outlook 2020 – Analysis - IEA." Accessed: Jun. 16, 2024. [Online]. Available: https://www.iea.org/reports/world-energy-outlook-2020

[5] R. Bender *et al.*, "Corrosion challenges towards a sustainable society," *Materials and Corrosion*, vol. 73, no. 11, pp. 1730–1751, Nov. 2022, doi: 10.1002/maco.202213140.

[6] M. Diantoro, T. Suprayogi, A. Hidayat, A. Taufiq, A. Fuad, and R. Suryana, "s Equation Fit Analyses for Solar Cell Parameters from I-V Curves," 2018, doi: 10.1155/2018/9214820.

[7] "(2) (PDF) Proiect de cercetare științifică: Cercetări privind integrarea surselor fotovoltaice în rețelele electrice." Accessed: Jun. 22, 2024. [Online]. Available: https://www.researchgate.net/publication/281522061_Proiect_de_cercetare_stiintifica_Cercetari_privind_integrarea_surselor_fotovoltaice_in_retelele_electrice/figures?lo=1

[8] "Solar cells: Operating principles, technology, and system applications - NASA/ADS." Accessed: Jun. 22, 2024. [Online]. Available: https://ui.adsabs.harvard.edu/abs/1982ph...book.....G/abstract

[9] "Meteo Data Source – PVsyst." Accessed: Jun. 22, 2024. [Online]. Available: https://www.pvsyst.com/meteo-data-source/

[10] "Investeşte în oameni !"

[11] M. Bălăceanu, N.-S. Popa, V. Nae, M.-C. Târhoacă, and M.-O. Popescu, "The Influence of Environmental Factors on a Photovoltaic Panel-PVsyst Simulation," *Automatica (EEA)*, vol. 72, no. 2, pp. 3–12, 2024, doi: 10.46904/eea.24.72.2.1108001.

[12] M. Bălăceanu, N.-S. Popa, V. Nae, M.-C. Târhoacă, and C. Popa, "State of the Art in Wind Turbine and Photovoltaic Panels." [Online]. Available: www.techniumscience.com

[13] N. Badara *et al.*, "'Mircea cel Batran' Naval Academy Scientific Bulletin, Volume XX-2017-Issue 1 The journal is indexed in: PROQUEST / DOAJ / Crossref / EBSCOhost / INDEX COPERNICUS / DRJI / OAJI / JOURNAL INDEX / I2OR

/ SCIENCE LIBRARY INDEX / Google Scholar / Academic Keys/ ROAD Open Access / Academic Resources / Scientific Indexing Services / SCIPIO / JIFACTOR 2017-Issue no. 1 ABSTRACT MECHANICAL AND ELECTRICAL SCIENCE."

[14] C. Schwingshackl *et al.*, "Wind effect on PV module temperature: Analysis of different techniques for an accurate estimation," in *Energy Procedia*, Elsevier Ltd, 2013, pp. 77–86. doi: 10.1016/j.egypro.2013.08.010.

[15] F. Chiacchio, F. Famoso, D. D'Urso, S. Brusca, J. I. Aizpurua, and L. Cedola, "Dynamic Performance Evaluation of Photovoltaic Power Plant by Stochastic Hybrid Fault Tree Automaton Model," *Energies 2018, Vol. 11, Page 306*, vol. 11, no. 2, p. 306, Jan. 2018, doi: 10.3390/EN11020306.

[16] R. S. Faranda, H. Hafezi, S. Leva, M. Mussetta, and E. Ogliari, "The optimum PV plant for a given solar DC/AC converter," *Energies (Basel)*, vol. 8, no. 6, pp. 4853–4870, 2015, doi: 10.3390/EN8064853.

[17] F. Famoso, R. Lanzafame, S. Maenza, and P. F. Scandura, "Performance comparison between micro-inverter and string-inverter Photovoltaic Systems," *Energy Procedia*, vol. 81, pp. 526–539, Dec. 2015, doi: 10.1016/J.EGYPRO.2015.12.126.

[18] "Energies | Free Full-Text | Dynamic Performance Evaluation of Photovoltaic Power Plant by Stochastic Hybrid Fault Tree Automaton Model." Accessed: Jun. 23, 2024. [Online]. Available: https://www.mdpi.com/1996-1073/11/2/306

[19] "Sci-Hub | A thermal model for photovoltaic panels under varying atmospheric conditions. Applied Thermal Engineering, 30(11-12), 1488–1495 | 10.1016/j.applthermaleng.2010.03.012." Accessed: Jun. 24, 2024. [Online]. Available: https://sci-hub.se/10.1016/j.applthermaleng.2010.03.012

[20] G. G. Singh, P. K. Dash, and N. C. Gupta, "Effect of Temperature on Power Output from Different Commercially available Photovoltaic Modules," 2015. [Online]. Available: www.ijera.com

[21] A. Hm, S. Klaus, J. Olindo, I. René, A. Van Swaaij, and M. Zeman, "Solar energy The physics and engineering of photovoltaic conversion, technologies and systems."

[22] G. Soni and A. Sharma, "Implementation of Heart Beat Sensor using DAQmx USB 6008," in *Proceedings of International Conference on Technological Advancements and Innovations, ICTAI 2021*, Institute of Electrical and Electronics Engineers Inc., 2021, pp. 207–211. doi: 10.1109/ICTAI53825.2021.9673336.

[23] "NEW NATIONAL INSTRUMENTS NI USB-6008 Data Acquisition Card | eBay." Accessed: Jun. 30, 2024. [Online]. Available: https://www.ebay.com/itm/314948491899